World Academy of Science, Engineering and Technology
International Journal of Mathematical and Computational Sciences
Vol:11, No:8, 2017

Fourier Galerkin Approach to Wave Equation with Absorbing Boundary Conditions

Alexandra Leukauf, Alexander Schirrer, Emir Talic

International Science Index, Mathematical and Computational Sciences Vol:11, No:8, 2017 waset.org/Publication/10007741

***Abstract*—**Numerical computation of wave propagation in a large domain usually requires significant computational effort. Hence, the considered domain must be truncated to a smaller domain of interest. In addition, special boundary conditions, which absorb the outward travelling waves, need to be implemented in order to describe the system domains correctly. In this work, the linear one dimensional wave equation is approximated by utilizing the Fourier Galerkin approach. Furthermore, the artificial boundaries are realized with absorbing boundary conditions. Within this work, a systematic work flow for setting up the wave problem, including the absorbing boundary conditions, is proposed. As a result, a convenient modal system description with an effective absorbing boundary formulation is established. Moreover, the truncated model shows high accuracy compared to the global domain.

***Keywords*—**Absorbing boundary conditions, boundary control, Fourier Galerkin approach, modal approach, wave equation.

I. Introduction

FROM acoustics to seismology, wave propagation is significant in many technical areas and its reliable simulation requires special care. One of the most common issues one has to deal with are large computational costs. They emerge when simulating the propagation of waves in very large domains and it is desirable to keep them to a minimum. To achieve this objective, it is necessary to truncate the simulation domain. The artificially generated boundaries cannot be treated like clamps, because spurious reflections would be generated, compromizing the interior solution. This undesirable phenomenon can be explained by the energy of the wave, bounded by the local domain [1]. In order to enable this energy to pass through the artificial boundaries, one must introduce specific boundary conditions, which can be realized in form of absorbing or transparent boundary conditions.

The need of finding *absorbing boundary conditions* (ABCs) for specific wave propagation problems increased quickly in the last few decades. Even though computing power has increased rapidly, the complexity of models has risen too, as well as the need for real-time capable models. Therefore, the development of highly efficient models is vital to meet real-time requirements. One example of practical usage can be found in rail traffic, whereby the complex pantograph/catenary interaction must be modeled and simulated carefully, even under real-time requirements. Highly efficient catenary models are required to enable real-time test bed scenarios with high fidelity. In [2], the catenary dynamics are modelled by utilizing the finite element method, using a moving-coordinate formulation and implementing wave-absorbing boundary layers. In [3], Facchinetti and co-authors use the classical Fourier approach to obtain a real-time capable catenary model. To minimize the spurious reflection at the boundaries, Facchinetti introduced a "forward shifting" approach, whereby the pantograph and the solution are periodically shifted, so that the moving pantograph remains sufficiently far away from the artificial boundaries. In this paper, a combination of ABCs and the Fourier approach as a basic method for a novel simulation approach is devised.

Real-time capable simulations and the optimization of computational costs are fundamental factors that have encouraged the investigation of boundary conditions for specific discretization schemes in the recent years. Engquist and Majda [4] developed perfectly absorbing non-local boundary conditions, approximated by local ones. In [1], Clayton and Engquist presented ABCs based on paraxial approximations and separated the energy of the outward-moving wave from that of the incoming wave. Guo and Shao [5] constructed an observer-based feedback scheme by only utilizing displacement measurements. Another example is to introduce a damped layer [6], [7], dissipating the energy of the out-travelling waves. Further approaches [8], [9] are based on Berengers perfectly-matched layer [10], whereby a lossy, anisotropic layer is derived at the boundaries to absorb the out-going waves.

In this work, the linear wave equation is discretized by utilizing the Fourier Galerkin approach. Unlike spatial discretization methods, such as the finite-element-method or the finite-difference-method, which discretize *partial differential equations* (PDEs) locally, the Fourier Galerkin approach discretizes globally via Fourier series. Due to orthogonality properties of the Fourier series, the PDE of the wave problem can be decoupled in space and time, which leads to a system of *ordinary differential equations* (ODEs), only depending on time. These ODEs can be efficiently solved for every eigenmode and the solution only needs to be transformed back to space-time-description. The accuracy of the approximated solution increases with the number of considered eigenmodes. For solving the wave problem with ABCs, this complex problem with inhomogeneous, dynamic boundary functions is split into a homogeneous and an inhomogeneous solution.

The methodology of this paper starts with basic information about the one-dimensional linear wave equation and continues with considering the homogeneous sub-problem. The subsequent part describes how the Fourier Galerkin approach can be used for modelling the wave problem, followed by the implementation of the ABCs and an

Alexandra Leukauf is mechanical engineering student at Technische Universität Wien, Vienna, Austria (e-mail: e1226357@student.tuwien.ac.at).
Alexander Schirrer and Emir Talic are with the Institute of Mechanics and Mechatronics, Technische Universität Wien, Vienna, Austria (e-mail: alexander.schirrer@tuwien.ac.at).

International Science Index, Mathematical and Computational Sciences Vol:11, No:8, 2017 waset.org/Publication/10007741

assembly of all required equations. As a final step, the back transformation of the total solution into space and time is outlined. After the methodology sections, the results for specific simulation test scenarios are illustrated, whereby the accuracy of the truncated system's solution depending on the initial field's shortest wavelength and the number of eigenmodes is studied.

II. Methodology

A. The One-Dimensional Linear Wave Equation

Regardless of whether one deals with the propagation of acoustic, electromagnetic or water waves - due to the wave equation, satisfactory simulation results can be achieved in many cases. This equation in its linearized form is a very important and equally one of the simplest second-order PDEs in physics. The approach developed in this paper is illustrated by the one dimensional linear scalar wave equation, given by

$$\frac{\partial^2 u(x,t)}{\partial t^2} - c^2 \frac{\partial^2 u(x,t)}{\partial x^2} = f(x,t). \tag{1}$$

with the boundary conditions

$$u(0,t) = u_0(t), t \geq 0 \tag{2}$$

$$u(L,t) = u_L(t), t \geq 0 \tag{3}$$

and the initial conditions

$$u(x,0) = g(x) \tag{4}$$

$$\dot{u}(x,0) = f(x). \tag{5}$$

Here, the parameter $c > 0$ is the constant wave propagation speed and $f(x,t)$ is the source function. Derivatives with respect to time t are denoted by a dot and spatial derivatives are denoted by a prime. The spatial coordinate $x \in \Omega$ is horizontal in direction of the wave propagation and it is defined in $\Omega \in [0, L]$. The field u may, for example, characterize the vertical deflection of a vibrating string, whereas u_0 and u_L are the boundary functions at the left and right boundaries. Equations (1)-(5) define a well-posed wave-propagation problem, for which a unique solution can be found. To solve this problem, it is divided into a homogeneous sub-problem and a boundary term, and the solutions of both sub-problems are superimposed.

B. The Homogeneous Sub-Problem

The homogeneous wave equation in one dimension can be illustrated by a vibrating string, which is fixed on both boundaries. The mathematical description of this homogeneous problem is given by

$$\frac{\partial^2 u_H(x,t)}{\partial t^2} - c^2 \frac{\partial^2 u_H(x,t)}{\partial x^2} = 0 \tag{6}$$

with the boundary conditions

$$u_H(0,t) = 0 \tag{7}$$

$$u_H(L,t) = 0, \tag{8}$$

and the initial conditions

$$u_H(x,0) = g(x) \tag{9}$$

$$\dot{u}_H(x,0) = f(x). \tag{10}$$

Imagining this string to be plucked, the initial displacement divides into two waves of the half amplitude, one wave moving in the left direction, the other one in the right direction. When an outward moving wave reaches the end of the string, the wave is reflected and inverted at the homogeneous Dirichlet boundary conditions (9) and (10).

The wave equation (6) can also be formulated as an operator factorization

$$\Big(\frac{\partial}{\partial t} - c\frac{\partial}{\partial x}\Big)\Big(\frac{\partial}{\partial t} + c\frac{\partial}{\partial x}\Big)u_H = 0, \tag{11}$$

whose general solution is of the form

$$u(x,t) = g_1(x + ct) + g_2(x - ct). \tag{12}$$

Thereby, g_1 and g_2 are two arbitrary, twice differentiable functions of a single variable [11, p.33-34], where g_1 is the solution of the first term and g_2 is the solution of the second term of (11). Moreover, solutions of either

$$\Big(\frac{\partial}{\partial t} - c\frac{\partial}{\partial x}\Big)u_H = 0 \tag{13}$$

as

$$\Big(\frac{\partial}{\partial t} + c\frac{\partial}{\partial x}\Big)u_H = 0 \tag{14}$$

are also solutions of (6). The first term $g_1(x + ct)$ of (12) represents wave components travelling to the left, whereas the second term characterizes the right-moving components. In order to calculate a satisfying approximation of the exact solution of the homogeneous wave problem, the Fourier Galerkin approach is introduced.

C. Fourier Galerkin Approach

The objective of utilizing the Fourier Galerkin approach here is to approximate (6) by a system of ODEs. Therefore, $u_H(x,t)$ will be approximated by

$$u_H(x,t) \doteq \sum_{k=1}^{k_{max}} u_{\mathrm{H},k}(t) \sin(\mu_k x), \tag{15}$$

where $k_{\max}$ represents the number of considered eigenmodes, which affects the accuracy of the approximate solution. In anticipation of the overall problem, the approximation of the source function $f(x,t)$ should be also mentioned here by

$$f(x,t) \doteq \sum_{k=1}^{k_{max}} f_k(t) \sin(\mu_k x). \tag{16}$$

Due to this approach, the solution is separated into time-depending and time-invariant parts. As a consequence, the derivatives with respect to both time and space simplify to

$$\ddot{u}_H(x,t) \doteq \sum_{k=1}^{k_{max}} \ddot{u}_{\mathrm{H},k}(t) \sin(\mu_k x) \tag{17}$$

International Science Index, Mathematical and Computational Sciences Vol:11, No:8, 2017 waset.org/Publication/10007741

$$u''_H(x,t) \doteq -\sum_{k=1}^{k_{max}} \mu_k^2 u_{\mathrm{H},k}(t)\sin(\mu_k x). \tag{18}$$

Inserting (17) and (18) into (6) leads to

$$\sum_{k=1}^{k_{max}} \left[\, \ddot{u}_{\mathrm{H},k}(t) + c^2\mu_k^2 u_{\mathrm{H},k}(t)\right] \sin\left(\mu_k x\right) = 0. \tag{19}$$

With respect to the homogeneous sub-problem, an equation for μ_k that complies with the homogeneous boundary conditions (7) and (8) is given by

$$\mu_k = \frac{k\pi}{L}, \tag{20}$$

which describes the k-th eigenmode. Using the orthogonality property of the Fourier series,

$$\int_0^L \sin(\frac{n\pi}{L}x)\sin(\frac{m\pi}{L}x)\,\mathrm{d}x = \frac{L}{2}\delta_{nm}, \tag{21}$$

where δ_{nm} is the Kronecker delta, (19) can be simplified to

$$\ddot{u}_{\mathrm{H},k}(t) + c^2\mu_k^2 u_{\mathrm{H},k}(t) = 0 \tag{22}$$

with $k = 1, ..., k_{\max}$. Finally, the initial conditions are obtained as

$$u_{\mathrm{H},k}(0) = \frac{2}{L}\int_0^L g(x)\sin(\mu_k x)\,\mathrm{d}x \tag{23}$$

and

$$\dot{u}_{\mathrm{H},k}(0) = \frac{2}{L}\int_0^L f(x)\sin(\mu_k x)\,\mathrm{d}x. \tag{24}$$

Thus, the homogeneous solution $u_{\mathrm{H}}(x,t)$ can be calculated, which is the first term of the total solution

$$u(x,t) = u_H(x,t) + u_0(t)\Big(1-\frac{x}{L}\Big) + u_L(t)\frac{x}{L} \tag{25}$$

of the problem (1)-(5). Due to (25), the behaviour at the boundaries is taken into account by superposing the homogeneous solution u_H and the solution for the boundaries u_0 and u_L.

D. Implementation of Absorbing Boundary Conditions

As illustrated in (11), the wave equation can be described by an operator factorization, whereas one term models the wave movement to the right, the other term describes the left moving wave. First, both bracket terms of (11) are considered separately.

$$\frac{\partial u}{\partial t} - c\frac{\partial u}{\partial x} = 0\Big|_{x=0} \tag{26}$$

$$\frac{\partial u}{\partial t} + c\frac{\partial u}{\partial x} = 0\Big|_{x=L} \tag{27}$$

Starting from (25), the derivatives with respect to time

$$\dot{u}(x,t) = \sum_{k=1}^{k_{max}} \dot{u}_{\mathrm{H},k}(t)\sin(\mu_k x) + \dot{u}_0(t)\Big(1-\frac{x}{L}\Big) + \dot{u}_L(t)\frac{x}{L} \tag{28}$$

$$\ddot{u}(x,t) = \sum_{k=1}^{k_{max}} \ddot{u}_{\mathrm{H},k}(t)\sin(\mu_k x) + \ddot{u}_0(t)\Big(1-\frac{x}{L}\Big) + \ddot{u}_L(t)\frac{x}{L} \tag{29}$$

as well as the spatial derivatives u' and u''

$$u'(x,t) = \sum_{k=1}^{k_{max}} u_{\mathrm{H},k}(t)\mu_k\cos(\mu_k x) - u_0\frac{1}{L} + u_L\frac{1}{L} \tag{30}$$

$$u''(x,t) = -\sum_{k=1}^{k_{max}} u_{\mathrm{H},k}(t)\mu_k^2\sin(\mu_k x) \tag{31}$$

must be derived for later calculation steps. Inserting (28) and (30) into (26) and (27) leads to

$$\dot{u}_0 = c\Big[\sum_{k=1}^{k_{max}} u_{\mathrm{H},k}\mu_k - \frac{1}{L}u_0 + \frac{1}{L}u_L\Big] \tag{32}$$

for the left boundary and

$$\dot{u}_L = -c\Big[\sum_{k=1}^{k_{max}} u_{\mathrm{H},k}\mu_k(-1)^k - \frac{1}{L}u_0 + \frac{1}{L}u_L\Big] \tag{33}$$

for the right boundary. When merging (29) and (31) with the wave equation (1), one gets

$$\begin{aligned}\sum_{k=1}^{k_{max}} \ddot{u}_{\mathrm{H},k}\sin(\mu_k x) + \ddot{u}_0\Big(1-\frac{x}{L}\Big) + \ddot{u}_L\frac{x}{L} \\ +c^2\sum_{k=1}^{k_{max}} u_{\mathrm{H},k}\mu_k\sin(\mu_k x) = \sum_{k=1}^{k_{max}} f_k\sin(\mu_k x)\end{aligned} \tag{34}$$

In (34), the second derivatives of the boundary functions appear, which can be derived by (32) and (33)

$$\ddot{u}_0 = c\Big[\sum_{k=1}^{k_{max}} \dot{u}_{\mathrm{H},k}\mu_k - \frac{1}{L}\dot{u}_0 + \frac{1}{L}\dot{u}_L\Big] \tag{35}$$

$$\ddot{u}_L = -c\Big[\sum_{k=1}^{k_{max}} \dot{u}_{\mathrm{H},k}\mu_k(-1)^k - \frac{1}{L}\dot{u}_0 + \frac{1}{L}\dot{u}_L\Big] \tag{36}$$

It can be seen that $\ddot{u}_0$ and $\ddot{u}_L$ are in dependence of $\dot{u}_0$ and $\dot{u}_L$. This circumstance leads to the necessity of adding the variables $\ddot{u}_0$ and $\ddot{u}_L$ to the system of equations and thus resulting in higher model complexity. To keep the computational costs to a minimum, $\dot{u}_0$ and $\dot{u}_L$, expressed in (32) and (33), are inserted into (35) and (36). After some calculations, the equations can be formulated by

$$\begin{aligned}\ddot{u}_0 = c\sum_{k=1}^{k_{max}} \dot{u}_{\mathrm{H},k}\mu_k - \frac{c^2}{L}\sum_{k=1}^{k_{max}} u_{\mathrm{H},k}\mu_k[1+(-1)^k] \\ +\frac{2c^2}{L^2}(u_0-u_L)\end{aligned} \tag{37}$$

$$\begin{aligned}\ddot{u}_L = -c\sum_{k=1}^{k_{max}} \dot{u}_{\mathrm{H},k}\mu_k(-1)^k \\ +\frac{c^2}{L}\sum_{k=1}^{k_{max}} u_{\mathrm{H},k}\mu_k[1+(-1)^k] - \frac{2c^2}{L^2}(u_0-u_L).\end{aligned} \tag{38}$$

International Science Index, Mathematical and Computational Sciences Vol:11, No:8, 2017 waset.org/Publication/10007741

The next step is to build the inner product of (34) with all considered eigenmodes by

$$\begin{aligned}\frac{2}{L}\Big[\int_0^L \ddot{u}_{\mathrm{H},k}\sin(\mu_k x)\sin(\mu_k x)\,\mathrm{d}x \\ + \int_0^L \ddot{u}_0(1-\frac{x}{L})\sin(\mu_k x)\,\mathrm{d}x + \int_0^L \ddot{u}_L\frac{x}{L}\sin(\mu_k x)\,\mathrm{d}x \\ + c^2\mu_k^2\int_0^L u_{\mathrm{H},k}\sin(\mu_k x)\sin(\mu_k x)\,\mathrm{d}x\Big] \\ = \frac{2}{L}\int_0^L f_k\sin(\mu_k x)\sin(\mu_k x)\,\mathrm{d}x.\end{aligned} \tag{39}$$

After further calculations and simplifications, this leads to

$$\ddot{u}_{\mathrm{H},k} + \frac{2}{k\pi}\ddot{u}_0 - \frac{2}{k\pi}(-1)^k\ddot{u}_L + c^2\mu_k^2 u_k = f_k. \tag{40}$$

Finally, $\ddot{u}_0$ and $\ddot{u}_L$ of (40) are eliminated by (37) and (38). Hence, all required equations for both sub-problems are outlined. Now, the original wave problem, including the ABCs, is described by

$$\begin{bmatrix}\dot{\boldsymbol{u}}_{\boldsymbol{H}}\\ \ddot{\boldsymbol{u}}_{\boldsymbol{H}}\\ \dot{u}_0\\ \dot{u}_L\end{bmatrix} = \underbrace{\begin{bmatrix}\boldsymbol{0} & \boldsymbol{I} & \boldsymbol{0} & \boldsymbol{0}\\ \boldsymbol{A} & \boldsymbol{B} & \boldsymbol{c} & -\boldsymbol{c}\\ \boldsymbol{c\mu_k^T} & \boldsymbol{0^T} & -\frac{c}{L} & \frac{c}{L}\\ \boldsymbol{d^T} & \boldsymbol{0^T} & \frac{c}{L} & -\frac{c}{L}\end{bmatrix}}_{M}\begin{bmatrix}\boldsymbol{u}_{\boldsymbol{H}}\\ \dot{\boldsymbol{u}}_{\boldsymbol{H}}\\ u_0\\ u_L\end{bmatrix} + \begin{bmatrix}\boldsymbol{0}\\ \boldsymbol{f_k}\\ 0\\ 0\end{bmatrix}, \tag{41}$$

where the entries of the $(2k_{\max}+2)\times(2k_{\max}+2)$ square matrix M are given by

$$\begin{aligned}A_{m,n} = (-c^2\mu_m^2)\delta_{m,n} \\ + \frac{2c^2}{m\pi L}[1+(-1)^m]\sum_{n=1}^{k_{max}}\mu_n[1+(-1)^n]\end{aligned} \tag{42}$$

$$B_{m,n} = -\frac{2c}{m\pi}\Big[\sum_{n=1}^{k_{max}}\mu_n + (-1)^m\sum_{n=1}^{k_{max}}\mu_n(-1)^n\Big] \tag{43}$$

$$C_k = -\frac{4c^2}{k\pi L^2}(1+(-1)^k) \tag{44}$$

$$D_k = -(-1)^j c\mu_k \tag{45}$$

E. Back Transformation

When the system of equations in (41) is solved by an appropriate ODE solver, one gets a solution field consisting of the solution for each eigenmode k at all defined time steps. After a back transformation due to (15), the total solution (25) can be calculated. Fig. 1 clarifies the composition of the total solution $u(x,t)$. The upper plot shows each individual part of the solution, whereas the bottom plot depicts the total solution $u(x,t)$.

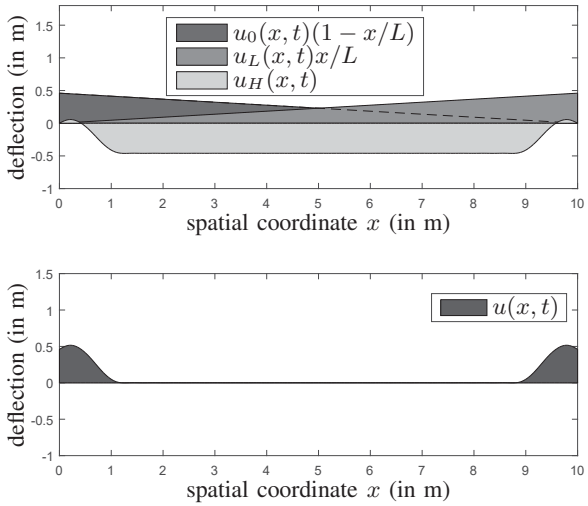

Fig. 1 Superposition of the solution components u_H (homogeneous sub-problem), u_0 (left boundary contribution) and u_L (right boundary contribution)

III. Results

To compare the Fourier Galerkin approach and other discretization methods in terms of model fidelity, the following test function, defined by

$$y(x,0) = e^{-(\frac{1}{a}(x-\frac{L}{2}))^2} \tag{46}$$

is used as the initial function $g(x)$ in (23) in the following simulation. The domain has total length $L=10$, and a is a factor proportional to the wavelength. At the deflection of 0.5 the initial function has a width of 2a. Fig. 2 shows a plot of the

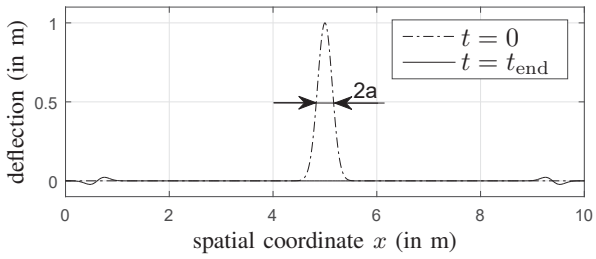

Fig. 2 Solution fields at times $t=0$ and $t=t_{\mathrm{end}}$ (after initial components ideally would have left the domain)

test function prescribed as initial displacement with $a=0.2$ and $k_{\max}=100$ eigenmodes. The peak in the middle of the string shows the test function at the beginning, which splits into a left and right wave peak of half amplitude. At time $t=t_{\mathrm{end}}$, the wave has travelled through the boundaries and a small amount of spurious reflections has occurred.

To quantify the absorption accuracy of the setup, the fit is defined by

$$f_A = \Big(1 - \frac{\|u(x,t=t_{\mathrm{end}})\|_{L_2}^2}{\|u(x,t=0)\|_{L_2}^2}\Big)\cdot 100\%, \tag{47}$$

International Science Index, Mathematical and Computational Sciences Vol:11, No:8, 2017 waset.org/Publication/10007741

utilizing the Euclidean norm

$$\|u(x)\|_{L_2}^2 = \int_0^L \big(u(x)\big)^2 \mathrm{d}x. \tag{48}$$

Here, the signal under the test function at $t = 0$ is compared to the area of the reflection after the test duration t_{end}. The test duration is chosen such that the wave has completely moved through the boundaries. Hence, the runtime depends on the wave propagation speed and the wavelength and is selected as

$$t_{\mathrm{end}} = \frac{1}{c}\Big(\frac{L}{2} + 3a\Big) \tag{49}$$

whereby c has no influence on the accuracy of the simulation. Fig. 3 gives some indication about the relations of the fit

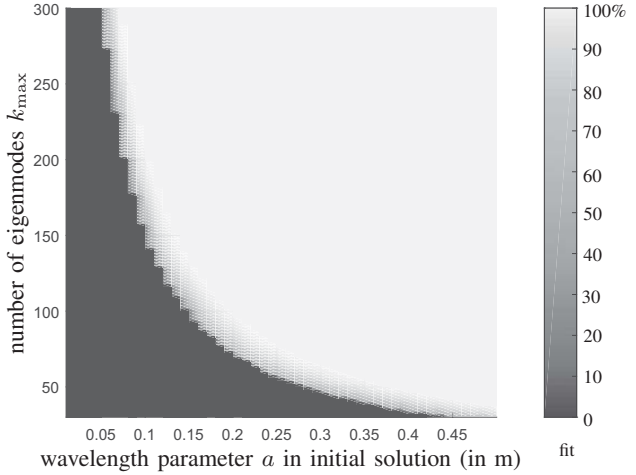

Fig. 3 The fit as an indicator for absorption quality, depending on the wavelength parameter a and the number of eigenmodes.

with the wavelength and the number of eigenmodes $k_{\max}$. The relation between the eigenmodes and the wavelength is prescribed by

$$\lambda_k = \frac{2\pi}{\mu_k}. \tag{50}$$

Hence, $k_{\max}$ determines the shortest resolved wavelength. From this plot one can infer, that the fit increases with more eigenmodes, as well as with lower frequencies present in the initial solution. In Fig. 4, the amplitude of the reflected wave is investigated. Therefore, the ratio h_r between the amplitude h of the test function at $t = 0$ and the amplitude of the reflections $h(t_{\mathrm{end}})$ is defined as

$$h_r = \frac{h(t_{\mathrm{end}})}{h(t=0)} \cdot 100\% \tag{51}$$

with

$$h(t) = \|u(x,t)\|_\infty = \max\|u(x,t)\|. \tag{52}$$

Now, h_r in dependence of the initial solution's wave length and the number of eigenmodes is plotted in Fig. 4. In the white area of the plot, the simulated results are unsatisfying, whereas in the dark grey area reflections of less than 2% of the initial amplitude can be achieved.

The plot in Fig. 5 can be seen as a vertical cross section of Fig. 3 for selected values a. Even though the fit tends to

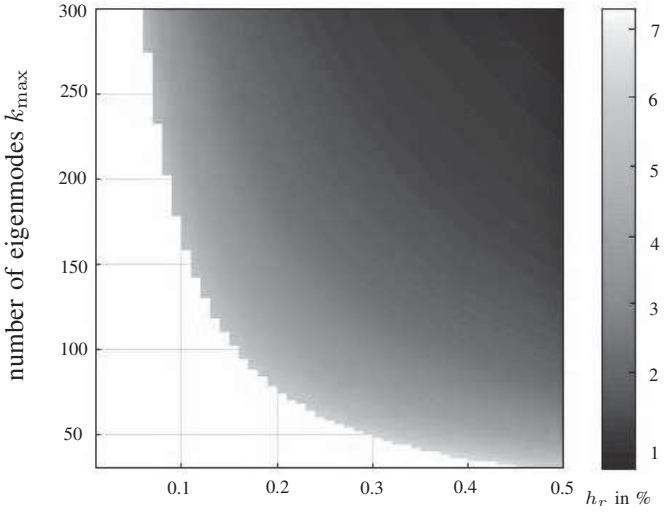

Fig. 4 The amplitude of reflections in dependence of the wavelength parameter a and the number of eigenmodes

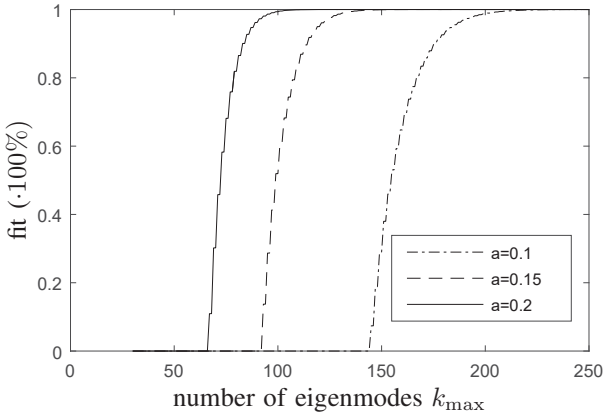

Fig. 5 The behaviour of the fit for specific wavelength parameters $a = 0.1, 0.15, 0.2$ in dependence of the number of eigenmodes

100% with an increasing number of eigenmodes, the speed of convergence decreases for a higher fit. As apparent from this plot, the speed of convergence also decreases with decreasing wavelength parameter a.

IV. Conclusion

This paper illustrates the application of the Fourier Galerkin approach for modelling the one dimensional wave problem and solving the general inhomogeneous problem. In addition, computational costs have been reduced by truncating the computational domain and introducing absorbing boundary conditions (ABCs) at the artificial boundaries, formulated in the Fourier Galerkin approximation. The necessity of ABCs arises from the fact that a wave cannot pass trough Dirichlet domain boundaries and thus, the wave is reflected. To avoid these spurious reflections, highly absorbing boundary functions have been implemented, which ensure a stable and accurate model for simulation.

The sections are organised in such a way that this paper can be used as a direct modus operandi for modelling the

International Science Index, Mathematical and Computational Sciences Vol:11, No:8, 2017 waset.org/Publication/10007741

wave problem with ABCs. First, some basic information of the wave equation are discussed and the homogeneous sub-problem is considered. Furthermore, the utilization of the Fourier Galerkin approach to the wave problem is outlined, as well as a systematic derivation and the implementation of the ABCs. Subsequently, the assembly of all necessary equations to a coupled system of ODEs of first order is shown and consequently the solution for each eigenmode and time step can be calculated. Finally, the back transformation to space and time is illustrated and the superposition of the homogeneous solution with the absorbing boundary functions is realized.

In order to ensure comprehensible results, a specific test function is applied, which is used in test simulations. The results of the test simulations show high accuracy, though the number of required eigenmodes increases rapidly with smaller wavelengths. Further research with regard to the optimization of the computational effort as well as the extension of this approach to other types of wave equations are planned.

In conclusion, using the Fourier Galerkin approach for the wave problem leads to an efficient simulation model with high fidelty for large wavelengths, however, the number of required eigenmodes and thus computational costs actually increase for smaller wavelengths.

REFERENCES

[1] R. Clayton and B. Engquist, "Absorbing boundary conditions for acoustic and elastic wave equations," *Bulletin of the Seismological Society of America*, vol. 67, no. 6, pp. 1529–1540, 1977. [Online]. Available: http://www.bssaonline.org/content/67/6/1529.abstract

[2] G. Aschauer, A. Schirrer, and S.-M. Jakubek, "Realtime-capable finite element model of railway catenary dynamics in moving coordinates," *IEEE Multi-Conference on Systems and Control*, 2016.

[3] A. Facchinetti, L. Gasparetto, and S. Bruni, "Real-time catenary models for the hardware-in-the-loop simulation of the pantograph–catenary interaction," *Vehicle System Dynamics*, vol. 51, no. 4, pp. 499–516, 2013.

[4] B. Engquist and A. Majda, "Absorbing boundary conditions for numerical simulation of waves," *Proceedings of the National Academy of Sciences*, vol. 74, no. 5, pp. 1765–1766, 1977. [Online]. Available: http://www.pnas.org/content/74/5/1765.abstract

[5] W. Guo and Z.-C. Shao, "Strong stability of an unstable wave equation by boundary feedback with only displacement observation," *IEEE Transactions on Automatic Control*, vol. 57, no. 9, pp. 2367–2372, 2012.

[6] C. Cerjan, D. Kosloff, R. Kosloff, and M. Reshef, "A nonreflecting boundary condition for discrete acoustic and elastic wave equations," *Geophysics*, vol. 50, no. 4, pp. 705–708, 1985.

[7] J. Sochacki, R. Kubichek, J. George, W.-R. Fletcher, and S. Smithson, "Absorbing boundary conditions and surface waves," *Geophysics*, vol. 52, no. 1, pp. 60–71, 1987.

[8] B. Chen, D.-G. Fang, and B.-H. Zhou, "Modified Berenger PML absorbing boundary condition for FD-TD meshes," *IEEE Microwave and Guided Wave Letters*, vol. 5, no. 11, pp. 399–401, 1995.

[9] D. Komatitsch and J. Tromp, "A perfectly matched layer absorbing boundary condition for the second-order seismic wave equation," *Geophysical Journal International*, vol. 154, no. 1, pp. 146–153, 2003.

[10] J.-P. Berenger, "A perfectly matched layer for the absorption of electromagnetic waves," *Journal of computational physics*, vol. 114, no. 2, pp. 185–200, 1994.

[11] W. A. Strauss, *Partial differential equations - An introduction*, second edition ed.